IEEE Access
Multidisciplinary ⋮ Rapid Review ⋮ Open Access Journal

Received 3 November 2023, accepted 12 January 2024, date of publication 22 January 2024, date of current version 9 February 2024.

Digital Object Identifier 10.1109/ACCESS.2024.3356790

RESEARCH ARTICLE

Are European Initiatives Related to Local Spectrum Allocation for Private 5G Networks Ready for Use in Industrial Cases?

LUIS M. BARTOLÍN-ARNAU[1], JOSE VERA-PÉREZ[1], VÍCTOR SEMPERE-PAYÁ[1,2], (Member, IEEE), AND JAVIER SILVESTRE-BLANES[1,3], (Member, IEEE)

[1]Instituto Tecnológico de Informática (ITI), 46022 Valencia, Spain
[2]Departamento de Comunicaciones (DCOM), Universitat Politècnica de València (UPV), 46022 Valencia, Spain
[3]Departamento de Informática de Sistemas y Computadores (DISCA), Universitat Politècnica de València (UPV), 03801 Alcoy, Spain

Corresponding author: Luis M. Bartolín-Arnau (lbartolin@iti.es)

This work was supported in part by MCIN/AEI/10.13039/501100011033 under Grant PID2021-123168NB-I00, in part by ERDF—A way of making Europe, and in part by the Generalitat Valenciana through the Instituto Valenciano de Competitividad Empresarial–IVACE and FEDER under Grant IMDEEA/2023/53.

This work involved human subjects or animals in its research. The authors confirm that all human/animal subject research procedures and protocols are exempt from review board approval.

ABSTRACT The introduction of the Factory of the Future has revolutionised the manufacturing sector through the integration of various technologies such as Automated Guided Vehicles (AGVs), Artificial Intelligence (AI), the Industrial Internet of Things (IIoT), cloud computing and cyber-physical control systems (CPCS). These advances have created the need to develop novel communication systems to support new industrial requirements. Therefore, the fifth generation of mobile networks (5G) has become one of the most relevant alternatives in this field. However, the current regulations in Europe and the spectrum reserved for private 5G may not be sufficient to meet the requirements of some of the industrial applications for which it was conceived. Therefore, it is necessary to analyse the private 5G network to identify the performance thresholds according to the requirements set by the 3rd Generation Partnership Project (3GPP) for the selected industrial scenarios. This work proposes a comprehensive analysis of the feasibility of private 5G infrastructures to meet the industrial requirements studied for different use cases proposed by 3GPP. For this purpose, laboratory tests have been carried out to analyse the performance of a 5G physical network infrastructure and the results were compared with those obtained after modelling different scenarios using Simu5G, a 5G simulator based on the OMNeT++ framework. The conclusions drawn from this work have shown that, although 5G technology is a key enabler for the industrial sector, there are European private spectrum reservation initiatives that do not have sufficient performance to meet the more restrictive requirements for different uses defined by 3GPP, and therefore need to be adapted to drive the adoption of new spectrum reservations for this type of private infrastructure in industry.

INDEX TERMS 3GPP, CPCS, cloud computing, private 5G networks, local spectrum, Simu5G, vertical domains.

I. INTRODUCTION

The impact of digitisation and automation in the industrial and manufacturing sector has led to the need for new communication systems, capable of supporting applications with very low latency and high data rates. From the perspective of Industry 4.0, the integration of different technologies, such as IIoT or CPCS, together with cloud computing and AI, have revolutionised the automation process in the industrial sector, as they have reduced human intervention in

The associate editor coordinating the review of this manuscript and approving it for publication was Xiali Hei.

manufacturing processes, increasing productivity and reducing occupational accidents [1], [2]. In industrial scenarios, wireless technologies are taking the lead due to their low installation costs and the high performance of the latest standards. Currently, there are wireless alternatives such as the latest variant of the IEEE802.11 standard, commercially known as Wi-Fi 6 [3], [4], which offers similar features to 5G technology, but at short range [5]. Therefore, the 5G technology developed by 3GPP, is a perfect candidate to enable the revolution of Industry 4.0 towards the concept of Industry 5.0 [6], where the adaptation of automation plays a key role in the revolution of the industrial sector [7]. Although the industrial manufacturing sector represents a variety of applications with different network requirements that are suitable for automation, 3GPP focuses on three types of service: enhanced Mobile Broadband (eMMB), which supports services with high data rates and high mobility radio access; massive Machine Type (mMTC), which is used for the transmission of rare, massive, and small packets with higher latency than the other two, resulting in low power consumption and long battery life; and Ultra-Reliable Low Latency Communication (URLLC), which is used for devices with extreme network reliability that communicate bidirectionally with low latency [8].

The criticality of data for businesses and the continuous provision of low-latency network access require 5G private networks [9]. In addition, this type of network provides a means to share data securely and autonomously, with flexibility and greater coverage than other wireless networks, making it a powerful industrial communications network. As a result, private 5G network deployments have grown exponentially to provide reliable and scalable solutions [10].

5G networks can operate in two frequency ranges, both in the sub-6 GHz range and in millimetre waves, called FR1 and FR2 respectively [11]. The advantages of using signals in the sub-6 GHz range, such as improved signal strength in adverse weather conditions, the ability of the waves to penetrate buildings or the ability to travel further than millimetre waves, make it more attractive to deploy 5G networks in industrial environments in the FR1 range. For this reason, the FR2 range is used to cover densely populated areas but over short distances, which is why the millimetre wave bands are preferred to the mass communication bands, which are susceptible to blocking due to their shorter transmission range [12].

In the case of EU countries, there are two groups that make different spectrum reservations for private networks. In the minority group, countries such as Finland, France and Spain, have a spectrum reservation in the n40 band (2300 - 2400 MHz) with a bandwidth of 20 MHz while the spectrum reserved by the majority group of countries such as UK, Germany, Poland, Switzerland and Sweden is in the n78 band (3300 - 3800 MHz) with a bandwidth of up to 100 MHz.

The allocation of spectrum and bandwidth for private networks, defined independently by each country, creates uncertainty in meeting the requirements specified by 3GPP [13] for the use cases of the two types of service. Due to these issues, analysing the feasibility of the private 5G network with respect to the requirements specified by 3GPP for different use cases in industrial environments is a key contribution of this work. Furthermore, the modelling of industrial scenarios with 5G communications and the validation of the critical requirements specified by 3GPP for the analysed use cases represent a comprehensive investigation to verify whether the current European trends regarding the local spectrum allocation for private 5G networks meet the necessary requirements demanded by new use cases in the emerging concept of industry, known as Industry 5.0.

In order to carry out the analysis of the operational thresholds of the physical infrastructure of the private 5G network, the communication between the end user equipment and the base station, referred to in 5G terminology as the User Equipment (UE) and the Next Generation Node B (gNB), respectively, is examined and evaluated. Different industrial use cases are modelled using the selected simulator and then the performance of the 5G network is verified after laboratory tests. When modelling the use cases, relevant parameters in the 5G network are varied, such as the message transfer interval between the UEs and the gNB, the size of the information packets or the resources allocated to the uplink (UL) and downlink (DL) traffic, taking into account the performance evaluation on both links. UL traffic is carried with 64-QAM channel modulation, since this is the modulation allowed by the UE. However, for DL traffic, 256-QAM modulation is used because it is the maximum modulation allowed by the gNB. The parameterisation of the modelled use cases follows the requirements specified by 3GPP.

Similarly, in [14], the E2E latency behaviour is studied through several simulations with a single radio resource allocation in the n40 band. For this purpose, Simu5G is used to vary other parameters of interest for the 5G network, such as the number of UEs, the message size or the transfer interval, for three applications detailed by 3GPP with different requirements.

Following on from the work in [14], we add a detailed analysis of the performance in the n78 band. Furthermore, the study of network parameters such as peak throughput, packet delivery ratio (PDR) and end-to-end latency (E2E) in the n40 band is extended. To this end, a laboratory testbed was set up and the results obtained were with those obtained from the use case modelling in Simu5G. In order to study in detail the performance of the selected spectrum reserve, various tests were carried out by modifying the allocation of the radio resources of the private 5G network favouring the type of traffic for each application. These results make it possible to characterise different types of industrial scenarios according to the type of traffic of the application, and thus to develop a variable allocation of the 5G network resources according to the type of traffic. In this way, it is analysed whether the current European initiatives on spectrum reservation are sufficient or whether additional work is needed for private

5G networks to meet the expectations of the Factory of the Future.

The rest of the work is organised as follows. Section II reviews related work on 5G network simulations in different environments and configurations. Section III presents an overview of a 5G network and, in detail, private 5G networks, as well as a brief analysis of spectrum reservation at the European level. Section IV presents the simulation environment used, while Section V focused at the physical network infrastructure and the performed scenarios. Section VI presents the evaluated tests and the industrial scenario configuration, highlighting the metrics of interest and discussing the results obtained from the simulations and the performed test of the physical 5G infrastructure. Finally, conclusions and future works are presented in Section VII.

II. RELATED WORK

Although there is a wide variety of 5G network simulators, such as the Vienna 5G SL simulator [15], 5G K-Simulator [16], 5G-LENA [17], 5G-air-simulator [18] and Py5cheSim [19], all of them have a number of drawbacks, such as not having tools to evaluate end-to-end scenarios or only focusing on simulating the MAC and PHY layers, among others [20]. However, Simu5G is a model library written on top of the OMNeT++ framework that uses the INET library to perform end-to-end simulation studies. In [20] the authors explain the operation and describe of the simulation library. The work also includes device-to-device transmissions and typical examples of scenarios involving mobile UEs in 5G networks. To evaluate this technology, parameters such as E2E latency or PDR are measured. Other work evaluates scenarios combining different technologies such as 5G-IoT [21], 5G-WiFi [22] or 5G-Openwifi [23]. Studies and tests of Multi-access Edge Computing (MEC) applications in 5G scenarios using the Simu5G library have also been presented, such as [24], [25], [26], and [27], but few works evaluate the operating thresholds of private 5G networks in industrial environments [14], [28], as they focus on the design and development of applications combining different wireless technologies with 5G communication [21], [22], [24], [25], or the development of novel applications such as F1TENTH, which enables 5G communication between road elements with Unmanned Aerial Vehicles (UAVs) and autonomous racing cars [29].

On the other hand, there are works that define possible theoretical architectures for private 5G networks [9], [30], but without developing any type of application, since they include the use cases referenced in the work itself by sectors such as manufacturing, healthcare and transport, among others.

In conclusion, there is great interest in the development and deployment of 5G technology, although the applicability of private 5G networks in an industrial environment has not been analysed. For this reason, it is necessary to evaluate the different spectrum and bandwidth reservation solutions for private networks presented by different European countries in order to verify and assess the thresholds for the operation of private 5G networks. Therefore, the most restrictive scenario has been chosen, as there is no homogeneous spectrum reservation for all European countries, as stated in the draft order on the 5G Action Plan adopted by the European Commission in [31].

III. 5G SPECIFICATION

The use of 5G networks enables several advantages such as longer communication distances, a larger number of connected devices, better performance of non-line-of-sight (NLOS) communication and better congestion control compared to other wireless technologies [5].

A. SERVICE-BASED ARCHITECTURE

At a high level, the main architectural elements of a 5G mobile network are the Radio Access Network (RAN) and the Core Network (CN). There are two possible architecture implementations in a 5G mobile network: a Non-Standalone (NSA) network, where the 5G RAN is exposed over an existing 4G LTE network. Instead, the Standalone (SA) network is a completely new mobile network architecture that requires a new 5G packet core that does not depend on any existing LTE infrastructure. The CN part is composed of one or more User Plan Functions (UPFs), which have the role of interconnection between the RAN and the data network [32]. In terms of the 5G core (5GC) Service Based Architecture (SBA), shown in Fig. 1, the gNB connects to the 5G core Access and Mobility Management Function (AMF) through the N2 interface for control plane signalling, and connects to the UPF through the N3 interface for user plan data transfer.

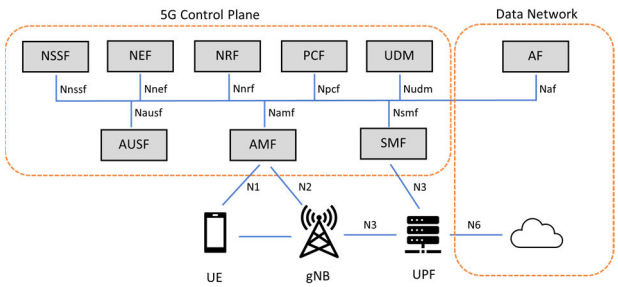

FIGURE 1. 5G service based architecture of cellular network.

Many of the advanced 5G features, including Network Function Virtualisation (NFV) and network fragmentation, will be managed in the core network, which is deployed as a building management system. The 5GC control plane consists of the following key components [33]:

- Network Slice Selection Function (NSSF)
- Network Exposure Function (NEF)
- Network Repository Function (NRF)
- Policy Control Function (PCF)
- Unified Data Management (UDM)
- Authentication Server Function (AUSF)
- Access and Mobility Management Function (AMF)

- Session Management Function (SMF)
- Application Function (AF)

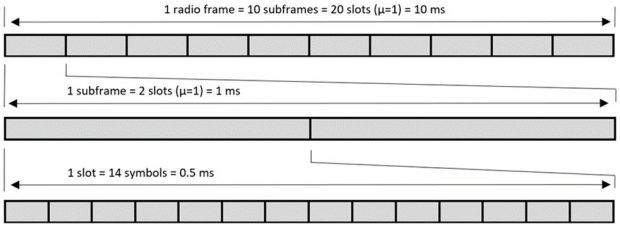

FIGURE 2. Radio frame, subframe and slots of 5G network.

B. FRAME STRUCTURE

As in LTE communications [34], the 5G radio frame has a duration of 10 ms and consists of 10 subframes of 1 ms duration each, as shown in Fig. 2. The number of slots in a subframe depends on the numerology index (μ) and is calculated as $N\_slots = 2^{\mu}$. The transmission time intervals (TTI) or duration of each slot is defined by μ as shown in Table 1. In addition, each slot has a total of 14 OFDM symbols if a normal cyclic prefix (CP) is used or 12 ODFM symbols if an extended CP is used; this case is only possible for a 60kHz ($\mu = 2$) subcarrier spacing (SCS) as shown in Table 2. Note that each subframe can be assigned individually depending on the 5G network traffic. Fig. 2 also shows as an example the partitioning of a 5G radio frame into different subframes and slots using a numerological index equal to one ($\mu = 1$).

TABLE 1. 5G numerology index sub-6 GHz, number of slots and TTIs [35].

μ	N_slots (per subframe)	TTI (ms)
0	1	1
1	2	0.5
2	4	0.125

TABLE 2. 5G numerology index sub-6 GHz – subcarrier spacing [11].

μ	$SCS = 2^{\mu} \cdot 15\ kHz$	Cyclic Prefix (CP)	Number of symbols
0	15	Normal	14
1	30	Normal	14
2	60	Normal, Extended	14, 12

As the value of the numerological index increases, so does the number of slots. Therefore, the duration of each slot and the duration of each symbol decreases. Consequently, the network throughput increases and the E2E latency decreases if the network is not saturated, since at that point the E2E latency increases exponentially and the network throughput decreases.

However, not all numerological index values are valid, as $\mu = 0,1,2$ is valid for frequencies in the sub-6 GHz range (FR1), as this frequency range is the focus of this work. On the other hand, $\mu = 2,3,4,5,6$ is for millimetre wave frequencies (FR2), although not all configurations are allowed. This all, depends on the bandwidth and the SCS used [36].

C. PHYSICAL LAYER 5G

The allocation of 5G physical layer resources depends on the mode of operation of the network. A 5G network supports both Frequency Division Duplex (FDD) and Time Division Duplex (TDD) modes of 5G communications. However, in this work, the TDD mode was used because it is the only one permitted for the n40 band [36]. Although there are many frequency bands for 5G networks, the n40 band was chosen because it is the band that Finland, France and Spain have reserved for private 5G networks.

On the other hand, there are many TDD patterns that deal with 3GPP predefined resource allocations [36]. These TDD patterns allocate resources based on the type of traffic (UL/DL). Such allocations cover different combinations, ranging from a radio resource allocation only for UL or DL, to mixed combinations depending on the traffic of the industrial application. In the case of the mixed combination, a guard period or flexible slot (FL) must be maintained between the allocation of radio resources for UL and DL traffic in the same 5G frame, as shown in Fig. 3. The purpose of this guard period is to minimise interference between UL/DL transmissions. It is good practice not to use of the flexible slot, such as the n40 band, centred on 2.4 GHz, which is a saturated spectrum with different technologies.

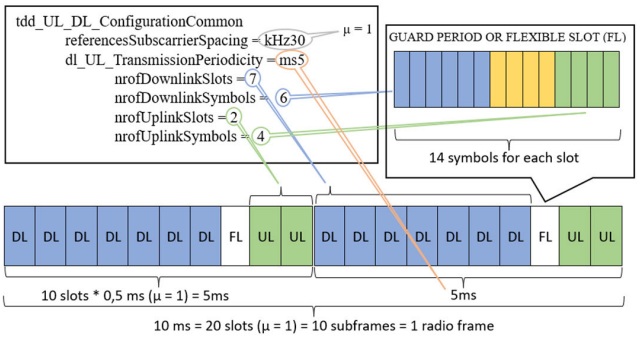

FIGURE 3. 3GPP TDD pattern 7 DL / 2 UL / 1FL example.

In addition, the theoretical calculation of the 5G radio channel throughput varies depending on the resource allocation for both UL/DL traffic, among other parameters. Therefore, different TDD configurations are tested in this work, as described in Section V.

As shown in (1) [37], both the modulation used and the bandwidth of the 5G network and thus the number of resource blocks (N_{PRB}^{BW}), affect the network throughput calculation. In addition, multiple-input multiple-output (MIMO) layers are also involved, which vary depending on the type of traffic and the size of the transport block (TB), which is defined by, among other parameters, the numerological index and the

bandwidth used.

$$\text{Data Rate (Mbps)} = \sum_{j=1}^{J} \left(v_{Layers}^{(j)} * Q_m^{(j)} * f^{(j)} * R_{max} * \frac{N_{PRB}^{BW(j),\mu} * 12}{T_s^{\mu} * 10^6} * \left(1 - OH^{(J)}\right) \right) \quad (1)$$

- J: number of aggregated component carriers in a band or band combination
- $v_{Layers}^{(j)}$: maximum number of supported MIMO layers. 8 for DL and 4 for UL [38].
- $Q_m^{(j)}$: maximum supported modulation and can take the values 2 for QPSK, 4 for 16QAM, 6 for 64QAM, 8 for 256QAM.
- $f^{(j)}$: scaling factor and can take values 1, 0.8, 0.75, and 0.4.
- R_{max} : depends on the type of coding from TS 38.212 [39] and TS 38.214 [40]
- μ : index numerology defined as TS 38.211 [41].
- T_s^{μ} : average OFDM symbol duration in a subframe for index numerology. Note that normal cyclic prefix is assumed. $T_s^{\mu} = 10^{-3}/(14 * 2^{\mu})$
- $N_{PRB}^{BW(j),\mu}$: maximum number of resource blocks allocation in bandwidth with index numerology, as defined in TS 38.101-1 [36]
- $OH^{(J)}$: overhead and takes the following values
  - 0.14, for frequency range FR1 for DL
  - 0.18, for frequency range FR2 for DL
  - 0.08, for frequency range FR1 for UL
  - 0.10, for frequency range FR2 for UL

D. PRIVATE 5G NETWORKS

In 3GPP terminology, a private 5G network is referred to as a non-public network (NPN) [42]. Thus, the public network (PN) would be the network that would be used by typical subscribers, and who would have a subscription with a mobile service provider (MSP).

Private 5G networks are virtual or physical cellular systems installed for private use by governments, businesses and other institutions, and include coverage areas of any size, from indoor to outdoor, small or large, mixing and matching different types of radios. They adapt to all types of sites and traffic conditions, even as their networks grow and expand. Private 5G networks can be deployed in fully private mode (i.e., on premises) and in hybrid mode (i.e., integrated with the MSP network), which may result in licensing [43] and, spectrum constraints or monthly subscription.

From a 3GPP perspective, there are two versions of NPN deployment, namely Standalone NPN (SNPN) and Public Network Integrated NPN (PNINPN) [44].

In this work, a SNPN, commercially known as a private 5G network, is deployed in a physically isolated and thus private manner, without the involvement of the network operator.

In the case of EU countries, there are two groups with different spectrum reservations for private networks. In the minority group, countries such as Finland, France and Spain, shown in blue in Fig. 4, have a spectrum reservation around the n40 band [36] in the FR1 range with a bandwidth of 20 MHz. However, in the case of Spain, if there is a nearby network of a public agency or companies dedicated to essential services, spectrum sharing is mandatory, reducing the bandwidth to 10 MHz. On the other hand, the majority group, made up of countries such as the United Kingdom, Switzerland, Germany, Poland and Sweden, among others, shown in green in Fig. 5, have a reserve of between 10 MHz and 100 MHz, in blocks of 10 MHz around the n78 band.

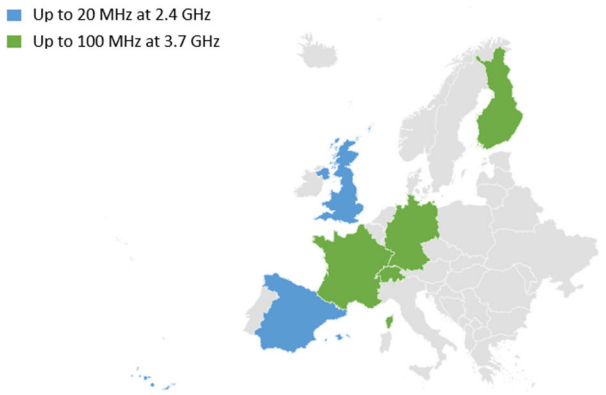

FIGURE 4. Local spectrum reservation for private networks for different European countries.

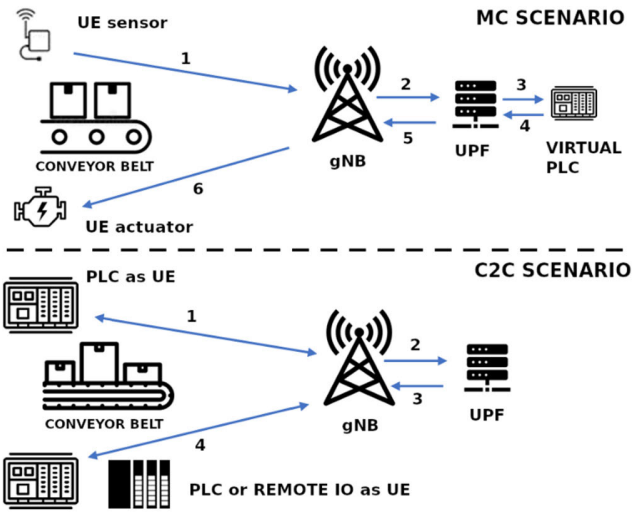

FIGURE 5. Cyber-physical control applications.

Due to government regulations and policies, 5G deployment is taking place at different paces and with certain characteristics that differ from country to country, as each country reserves different spectrum and bandwidth. Specifically, this paper focuses on an SNPN deployments with licensed spectrum, mainly in the n40 band.

The rest of the EU countries present diffuse information on spectrum reserves for private 5G networks in the FR1 range, while other countries focus on the FR2 range dedicated

to millimetre waves. For this reason, there are European countries that, while promoting the use of 5G, have not bet on private 5G networks, but have commercialised 5G spectrum reserves with large telcos.

IV. 5G SIMULATION FRAMEWORKS

This section explains the OMNeT++ simulation framework and how the Simu5G libraries simulate the data plane of a 5G network.

A. THE OMNeT++ FRAMEWORK

OMNeT++ [45] is a discrete event simulation framework that can be used to model any type of network, including wired and wireless networks. OMNeT++ divides the simulation files into three parts. For the model behavior, C++ is used for the model behaviour, the model description is expressed in separate files written in Network Description Language (NED) and the parameter values are expressed in Initialisation (INI) files. The OMNeT++ software supports automated simulation [46], which facilitates the simulation programming steps. Of particular note is the model library for OMNeT++, called INET [47], which models a communications network with a large number of components, including models for the Internet stack (TCP, UDP, etc.), link layer protocols (Ethernet, PPP, etc.), and various customisable mobility models, Quality of Service (QoS) architectures, etc.

B. MODELLING 5G COMMUNICATIONS

Simu5G is a 5G simulation library for the OMNeT++ simulation framework. It contains a collection of models with interfaces that can be instantiated and connected to build complex simulation scenarios. Simu5G is compatible with the INET library, which allows the simulation of end-to-end scenarios using TCP/IP networks.

Simu5G models the 5G RAN and CN data planes [48]. It supports handover and inter-cell interference coordination. In addition, Simu5G supports both Frequency Division Duplex (FDD) and Time Division Duplex (TDD) modes of 5G communication. It also has a high granularity in terms of resource allocation in 5G networks for both uplink and downlink traffic by uniquely assigning the slot symbols of a 5G frame to a traffic type, thereby improving network performance. It also enables inter-cell interference coordination, carrier selection and energy efficiency, among others.

Simu5G models the physical transmission using realistic and customisable channel models. It also provides carrier aggregation, which can be used for multi-frequency communication of carrier components. In this thesis, the parameters of the NED and INI files have been parameterised to allow the choice of carrier frequencies, bandwidths and number of resource blocks. The numerology, which varies the spacing between subcarriers and the slot duration of the 5G signals, is also adjusted.

V. 5G INDUSTRIAL SCENARIO

The complex consists of an industrial plant with the necessary service area for the use of 50 UEs implementing an SNPN architecture for each of the applications described later with several automated processes. Specifically, two cyber-physical control applications are evaluated in this scenario. The first, Motion Control, and the second, Control to Control, hereafter referred to as MC and C2C. Table 3 shows the requirements in terms of E2E latency as specified by 3GPP [13], [14]. Note that these use cases are included in applications dedicated to process and factory automation in the context of the Factory of the Future.

TABLE 3. Requirements for cyber-physical control applications.

Use Case	E2E Latency Maximum	Message Size (Bytes)	Transfer Interval (ms)	# of UEs	Service Area
MC	< transfer interval	50	0.5 – 2	≤ 20	50 x 10 x 10 m
C2C	< transfer interval	1k	10	5-10	100 x 30 x 10 m

Communication services for factory automation have stringent requirements, and operation is limited to a relatively small service domain that does not require interaction with the public network [49].

For the next evaluations, some considerations have been assumed, such as the direct 5G connectivity of both the programmable logic controller (PLC) and the various peripherals or distributed devices considered in each industrial scenario.

Fig. 5 shows the two industrial scenarios considered, MC at the top and C2C at the bottom. The one-way communication of an MC scenario takes place between a sensor and an actuator, both acting as UEs. Depending on the information captured by the sensor, the PLC virtualised in the UPF makes the necessary decision and sends the order to the actuator. As shown in Fig. 5, UL traffic corresponds to arrows 1,2 and 3, while DL traffic corresponds to arrows 4,5 and 6, for an MC scenario.

In a C2C scenario, bidirectional communication takes place between two PLCs or a PLC and a remote IO system for a given process that share processing variables. In terms of transmission and networking, both use cases are quite similar, but the requirements for network performance and information exchange are completely different, as shown in Table 3. Furthermore, the communication process for the C2C scenario is carried out as shown at the bottom of Fig. 5, arrows 1 and 2 correspond to UL traffic while, arrows 3 and 4, correspond to DL traffic.

In order to homogenise the evaluation, the spectrum reserve for private networks offered by Finland, France and Spain has been used, as it is the most restrictive of the European Union initiatives in terms of bandwidth and because it is the reserved spectrum of the network deployed in the laboratory under evaluation. This reserved spectrum is concentrated in the n40 band and has a bandwidth of 20 MHz

with a subcarrier spacing of 30 kHz. In addition, a brief analysis of the reserved spectrum, mainly in Europe, centred on the n78 band with a bandwidth five times wider than the n40 band, is performed in order to compare the operation thresholds in the first test described in subsection V-C.

TABLE 4. Parameters described in *ini* file for Simu5G simulations.

Parameter Name	Value
# BS	1
Traffic	Depend on use case
Carrier frequency	2.4, 3.6 GHz
Scenario	Indoor Factory [50]
Bandwidth	20, 100 MHz
Service area	100 m x 100 m
Use TDD	Enabled
Fading + shadowing	Enabled
gNB TX Direction	Omnidirectional
gNB TX Power	46 dBm
gBN antenna gain	8 dBi
gNB noise figure	5 dB
UE TX Power	26 dBm
UE antenna gain	0 dBi
UE noise figure	7 dB
Number runs per configuration	10
Simulation time	60 s

A. CHARACTERISATION OF THE SIMULATION MODEL

Concerning the simulation framework, Table 4 shows the configuration file (also known as "ini" file in the Simu5G environment) containing the network parameters and their corresponding values. In addition, a random distribution of UEs is implemented in the industrial scenario and the traffic frames are sent periodically in each transfer interval on a case-by-case basis. Due to the variety of scenarios and zones of reflection, noise and interference generated in industrial environments, the communication is modelled as an indoor scenario, referred to by 3GPP as Indoor Factory [50]. As for the simulations, peak throughput, E2E latency and PDR results are obtained for each of the possible configurations. For this purpose, the transfer interval was varied between 2, 5 and 10 ms and, the packet size was varied between 10B, 20B, 50B, 100B, 200B, 500B, 1KB, 2KB and 3KB. In addition, 10 replicates were performed for each of the possible combinations, giving a total of 270 simulations per TDD frame configuration. It should be noted that the results shown for each possible combination have been calculated as the average of the ten values obtained.

The communication exchange starts at the UE side, which generates uplink traffic to be processed at the virtual server connected to the UPF for the MC use case. The UEs send a data message to the server at each transfer interval, defined by 3GPP as the time elapsed between the generation of two consecutive messages. Furthermore, the E2E latency calculation is performed from the time the UE sends the information frame until the processed UE response arrives from the server. It should be noted that the remaining parameters not listed in Table 4 have been left at their default values.

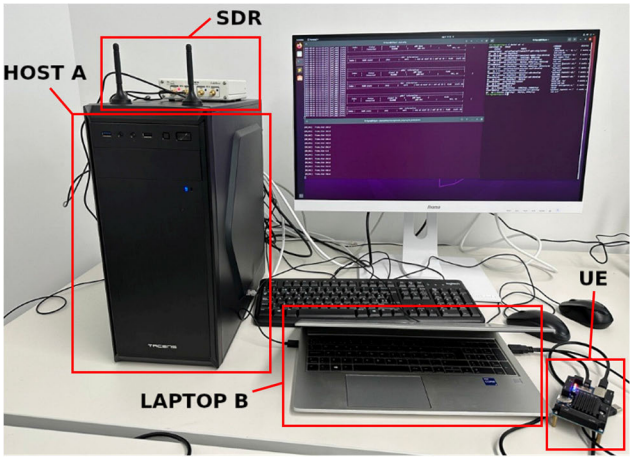

FIGURE 6. Components of the 5G network.

B. EXPERIMENTAL CONFIGURATION

A detailed description of the implemented 5G network prototype is given in Fig. 6. The components of the private 5G network are as follows:

- Host A is a desktop computer running the Ubuntu 18.04 Linux operating system on a 3.60 GHz 9th generation Intel Core™ i7 CPU with 16 GB of RAM and a 1 Gb/s Ethernet NIC. This device runs the core and gNB via the OpenAirInterface (OAI) optimised solution.

- The SDR USRP B210 implements the radio part of the gNB. It is connected to Host A via a USB 3.0 cable.

- The UE is a Quectel RMU500-EK with a M.2 RM500Q-GL modem connected to a laptop A via USB 3.0.

- Laptop B is a computer running the Microsoft Windows 11 Pro operating system on a 2.80 GHz 11th generation Intel Core™ i7 CPU with 32 GB of RAM and a 1 Gb/s Ethernet NIC. The Quectel RM500Q-GL modem was connected to this device via the USB 3.0 port.

OpenAirInterface configuration profiles are designed to perform the 5G network configurations described in the following tests. These profiles characterise all 5G network parameters, from the selected slot format to the carrier frequency. All this is done on Host A, which is responsible for running the components of the 5G CN part as well as the software part of the gNB.

However, due to the lack of equipment and in order to transmit the same traffic in both the simulated models and the 5G network, the physical UE transmits the same amount of traffic as the UEs in the simulations using the same transfer interval. Using each of the above methods, we were able to obtain the performance limits of the 5G architecture both in the modelling and in the 5G network located in the laboratory.

These lab tests are carried out using the *ping* and *iperf3* tools. These tests are performed bidirectionally between Host

A and Laptop B to obtain peak throughput thresholds for both UL and DL traffic.

TABLE 5. First test.

Sim. / Lab.	Frequency (GHz)	Band	Bandwidth (MHz)	Slot format
Sim.	2.4	n40	20	5 DL / 5 UL
Sim.	3.6	n78	100	5 DL / 5 UL
Lab.	2.4	n40	20	5 DL / 5 UL

C. TESTS PERFORMED

This section analyses the two tests carried out and detailed in Tables 5 and 6. Firstly, the performance of the two European spectrum pools described above is analysed. For this purpose, the same uniform slot configuration is maintained in resource allocation for both for UL and DL traffic, as shown in Table 5.

The first test aims to compare the operating thresholds in terms of peak throughput, E2E latency and PDR for the two European spectrum reservation initiatives for private 5G networks. As shown in Table 5, the first spectrum reservation focuses on a 2.4 GHz carrier frequency with a bandwidth of 20 MHz, while the second spectrum reservation focuses on a 3.6 GHz carrier frequency with a bandwidth of 100 MHz. However, they use the same TDD frame configuration. The numerological index used corresponds to a 30 kHz SCS. The slot format implemented is fair as it allocates the same number of slots to UL and DL traffic.

TABLE 6. Second test.

Sim. / Lab.	Frequency (GHz)	Band	Bandwidth (MHz)	Slot format
Sim.	2.4	n40	20	7 DL / 2 UL / 1 FL
Sim.	2.4	n40	20	3 DL / 6 UL / 1 FL
Lab.	2.4	n40	20	7 DL / 2 UL / 1 FL
Lab.	2.4	n40	20	3 DL / 6 UL / 1 FL

Having analysed the limitations of the 2.4 GHz (n40 band) spectrum reserve compared to 3.6 GHz (n78 band), the second test analyses the operating thresholds by setting the carrier frequency to 2.4 GHz and the bandwidth to 20 MHz. Note that only $\mu = 1$ is allowed in this band, as in the n78 band [36]. First, the slot format is prefixed by allocating more resources to DL traffic, while the second TDD frame configuration allocates more resources in favour of UL traffic. As shown in Table 6, the first TDD frame configuration consists of 7 DL slots, 2 UL slots and 1 FL slot, whereas, the second configuration consists of 3 DL slots, 6 UL slots and 1 FL slot, this being the configuration with a resource allocation in favour of UL traffic.

Finally, the operating thresholds obtained from the simulations are evaluated and compared with those obtained in the laboratory using the same slot format in favour of UL and DL traffic. The slot formats used are 3 DL / 6 UL / 1 FL and 7 DL / 2 UL / 1 FL, the latter being the standard resource allocation used for applications with DL traffic preference [29]. Therefore, the 2 DL / 7 UL / 1 FL slot format could not be tested and analysed as it requires at least 3 slots for DL, 2 for the channel state information reference signal (CSI-RS) and 1 for the synchronisation signal block (SSB), hence the 3 DL / 6 UL / 1 FL slot format is used.

The slot format assignments detailed in Table 6 therefore correspond to the massive burst DL or UL traffic, so that in each of the slot formats more slots are allocated to one type of traffic than the other. These configurations, which emulate two traffic extremes; when most of the traffic is DL or UL, analyse the performance thresholds of the 5G network in order to perform flexible resource allocation based on network traffic. Therefore, an important characteristic of these tests is that we analyse the performance of the 5G network for different radio resource allocations in order to evaluate the optimal configurations based on the industrial use cases described above.

VI. RESULTS AND DISCUSSION

The results obtained by applying the configurations described in the previous section are presented below. These configurations were applied to the industrial scenario described in Section V. The results are presented in the same order in which the tests designed in Section V-C are detailed.

The 5G network quality parameters for UL and DL traffic were investigated using three transfer intervals: 2 ms, 5ms, 10ms. These values have been chosen by the authors to be among the most restrictive defined by 3GPP. Different packet sizes were also used, ranging from 10 B to 3 KB. This provides a more granular analysis of the performance of a private 5G network. Furthermore, these results are evaluated and compared with the minimum requirements defined by 3GPP in Table 3 for two types of common industrial use cases such as MC and C2C.

A. FIRST TEST

Firstly, the results obtained of the modelling of the previous use cases are explained, followed by a detailed description of the results of the 5G network deployment in our laboratory.

The first test involves analysing the differences in the operating thresholds for the two European spectrum reservation initiatives. To do so, the same order as in Table 5 is followed. First the tests are performed in the n40 band and then in the n78 band. Figs. 7, 8 and Tables 7, 8 show the results for the n40 band, while Figs. 9, 10 and Table 9 show the results for the n78 band. The results are analysed independently for each 5G network parameter investigated. It should be noted that the network performances obtained for a transfer interval of 5 ms are the only results that can be compared for the two types of tests, simulation, and laboratory, since this transfer interval coincides with the DL/UL periodicity interval for $\mu = 1$, as detailed in Fig. 3.

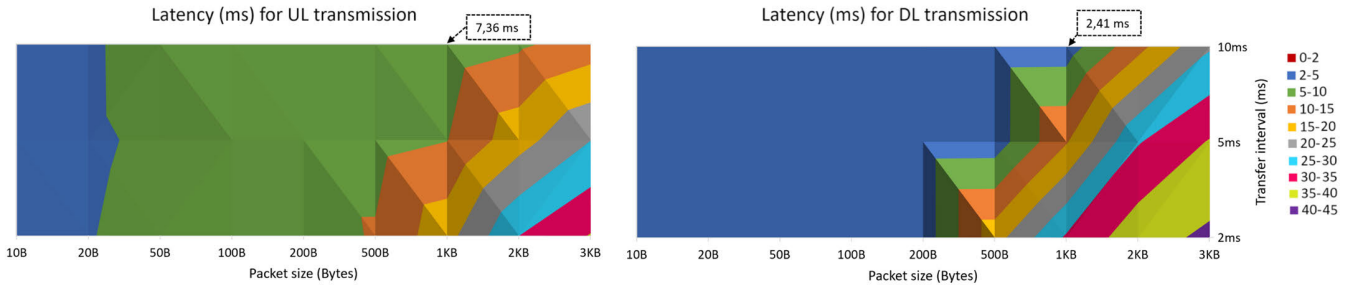

FIGURE 7. (Sim.) latency UL (left) and DL (right) for n40 band spectrum license.

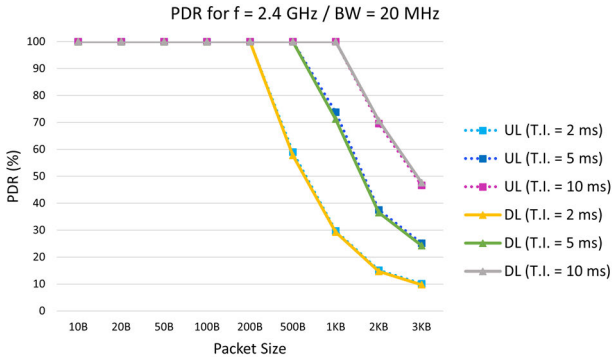

FIGURE 8. (Sim.) packet delivery ratio depending on the type of traffic for different transfer intervals for n40 band spectrum license.

TABLE 7. (Lab.) E2E latency and PDR results for the n40 band.

E2E latency (ms)			PDR (%)
Minimum	Average	Maximum	
6,35	10,51	16,25	100

Fig. 7 shows the latency for each packet size and transfer interval for the n40 band. A distinction is made between UL traffic (left) with 64-QAM channel modulation and DL traffic (right) with 256-QAM. These results show how the spectrum begins to saturate as the packet size increases. Additionally, differences in latency performance for different traffic types are also shown. 3GPP specifies in Table 3 that the E2E latency (UL+DL) must be lower than the transfer interval. Therefore, the spectrum reservation of the n40 band meets the requirements of the scenarios designed for a packet size of 1 KB and a transfer interval of 10 ms, resulting in 7.36 ms latency for UL traffic and 2.41 ms latency for DL traffic. In terms of E2E latency, this spectrum pool meets the requirements of the C2C use case, but does not meet the requirements of the MC use case, which has more restrictive requirements. This is because the E2E latency is limited by the modulation allowed by UE. In this case, a 64-QAM channel modulation for UL traffic is used.

On the other hand, Table 7 shows the experimental results of E2E latency and PDR obtained using the spectrum reserve at 2.4 GHz (n40 band). Comparing these results with Fig. 7, it is clear that there is no significant difference between the results obtained from simulations and laboratory tests when an average E2E latency of 10 ms is reached. However, the same is not true for the peak throughput. This is because the use of the OAI core [51] makes it impossible to manually select the modulation for each type of traffic. Instead, the 5G network itself chooses the modulation based on the Quality Indicator (QI). As a result, a peak throughput of 47.7 Mbps was achieved for DL traffic. This is similar to the values obtained in the simulation using 256-QAM modulation with a spectral efficiency of 7.41 [40]. The UL traffic reached a speed of 18.2 Mbps, which is much lower than the theoretical result. This is because the highest modulation that allowed a stable peak throughput is a BPSK with a spectral efficiency of 1.33 [40].

To conclude the analysis of spectrum licensing performance in the n40 band, Fig. 8 examines the PDR obtained for the previously selected transfer intervals and detailed message sizes. In addition, the PDR results obtained from the simulations distinguish between UL and DL traffic. With dashed lines and a square marker for UL traffic and a solid line and a triangular marker for DL traffic. It should be noted that by setting the same radio resource reservation for both types of traffic, the maximum message size that can be sent to obtain a PDR of 100% is similar for both types of traffic. Furthermore, when the transfer interval is increased, the maximum packet size that can be sent increases, while maintaining similar radio resources.

Fig. 9 is organised in the same way as Fig. 7, and shows the latencies for both UL (left) and DL (right) traffic obtained from the simulations for the n78 band. The spectrum reservation in the n78 band does not saturate as easily as in Fig. 7, which is mainly because the bandwidth of the reservation around n78 is five times larger than that centred on n40, as detailed in Table 5.

It is worth nothing that this spectrum reservation around the n78 band, although offering better performance than the n40 band reservation, does not meet the requirements of the MC use case, whereas for the C2C use case it offers a vast improvement in terms of message size, since for a 10 ms transfer interval the maximum message size is 3 KB without saturating the spectrum, although it is possible to further

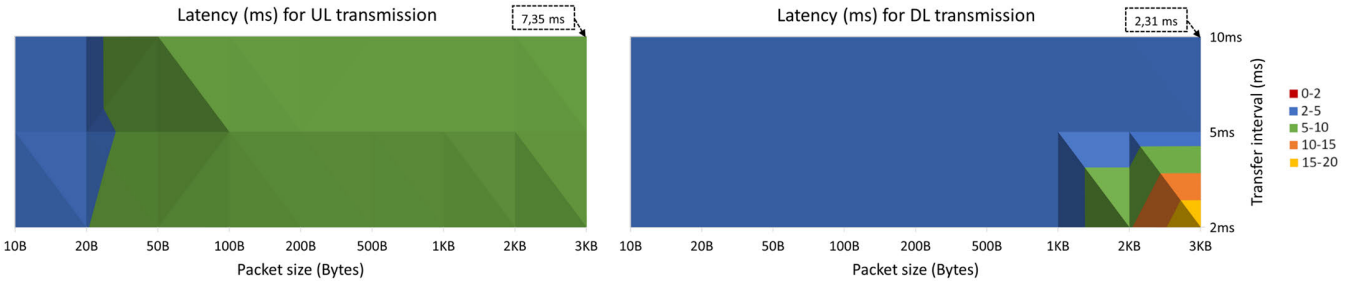

FIGURE 9. (Sim.) latency UL (left) and DL (right) for n78 band spectrum license.

increase the message size, but it is outside the scope of this work.

TABLE 8. Peak throughput for the n40 band.

Sim. / Theor. / Lab.	Transfer interval (ms)	Peak Throughput UL (Mbps)	Peak Throughput DL (Mbps)
Sim.	2 ms	48,13	48, 91
Sim.	5 ms	48,51	49,67
Sim.	10 ms	57,66	56,59
Theor.	5 ms	43,79	54,57
Lab.	5 ms	18,2	47,7

TABLE 9. Peak throughput for the n78 band.

Sim. / Theor.	Transfer interval (ms)	Peak Throughput UL (Mbps)	Peak Throughput DL (Mbps)
Sim.	2 ms	263,78	263,78
Sim.	5 ms	243,16	243,16
Sim.	10 ms	122,17	122,17
Theor.	5 ms	234,38	584,25

Tables 8 and 9 show the maximum performance achieved for the tests described in Table 5. Additionally, the theoretical results of the maximum performance are included under the abbreviation "Theor." using formula (1).

At a high level of analysis, it should be noted that the maximum throughput of the 5G network increases in the same proportion as the bandwidth. This is the reason why the maximum throughput, for a 5 ms transfer interval, is five times higher for the spectrum reservation around the n78 band than for the n40 band reservation.

However, in Table 9, the peak throughput for UL traffic obtained from the simulations is barely 10 Mbps different from the theoretical calculation but, for DL traffic, there are large differences between the results obtained from the simulations and the theoretical one. This difference is due to the fact that the n78 band spectrum is not saturated, as shown in Fig. 9 and, therefore, the throughput obtained in the simulations for DL traffic does not match the peak throughput of the 5G network.

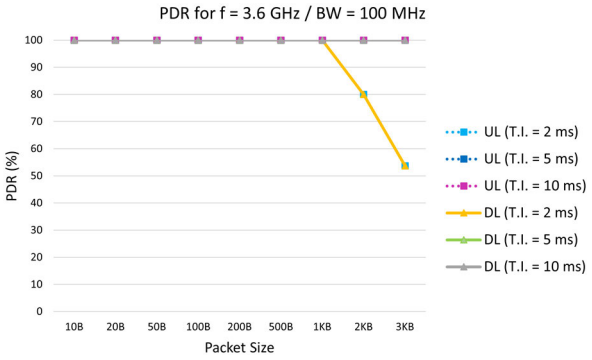

FIGURE 10. (Sim.) packet delivery ratio depending on the type of traffic for different transfer intervals for n78 band spectrum license.

To conclude the first test, the PDR obtained for the n78 band spectrum reservation initiative is examined. To this end, Fig. 10 shows the PDR results obtained from the simulations distinguishing between the two types of traffic for each of the three selected transfer intervals Also, for a transfer interval of 5 ms or higher, none of the selected packet sizes saturates the spectrum, allowing for further increase in message size. However, for a transfer interval of 2 ms, there is an operational threshold, as the maximum message size for UL and DL traffic is 1 KB.

Summarising this first detailed test in Table 5, it can be seen that the spectrum reservation around the n78 band has wider performance thresholds than the reservation centred on the n40 band. Furthermore, for the same transmission interval and without saturating the spectrum, the n78 band allows the transmission of message sizes three times larger than the maximum size allowed in the n40 band.

As expected, the maximum throughput increases with the bandwidth of the spectrum licence used. Finally, as the bandwidth of the spectrum licence increases, less spectrum is saturated and therefore the PDR results decrease more slowly.

B. SECOND TEST

The second test is aimed at analysing the operating thresholds of the private 5G network using configurations in favour of the two types of traffic. In this way, the optimal configuration for each industrial use case can be obtained according to the

type of traffic. The resource allocations are as detailed in Table 6. Note that for both latency and peak throughput, the results have been grouped by transfer interval and by traffic type. Figs. 11 and 12 and Tables 10 and 11 show the results of the simulations for the TDD pattern with 7 slots for DL traffic, 2 slots for UL traffic and 1 FL slot.

TABLE 10. E2E latency / PDR lab results for TDD pattern 7 DL / 2 UL / 1 FL.

E2E latency			PDR (%)
Minimum	Average	Maximum	
6,05	10,22	19,49	100

Fig. 11 shows the latencies for each of the selected transfer ranges and packet sizes, distinguishing between UL and DL traffic. The middle graph shows the E2E latency obtained for each transfer interval. With the exception of the bottom graph, the remaining graphs are notable for the logarithmic nature of the Y-axis, as very high latency values are obtained. In Fig. 11, the performance threshold of this TDD pattern shows an E2E latency of less than 10 ms for a message size of 500 B and a transmission interval of 10 ms.

It is worth noting that, by allocating more radio resources to DL traffic, it is observed that the latency results for DL traffic increase more slowly, whereas for UL traffic the latency increases very rapidly, reaching values above 200 ms.

On the other hand, Table 10 shows the experimental E2E and PDR latency results from the laboratory. Compared to Fig. 11, these results are very similar to the theoretical calculations and simulation results. However, while it may appear that an E2E latency of around 10 ms is sufficient for industrial environments, there are certain industrial use cases with more stringent throughput requirements, as detailed in Table 3.

TABLE 11. Peak throughput for TDD pattern 7 DL / 2 UL / 1 FL.

Sim. / Theor. / Lab.	Transfer interval (ms)	Peak Throughput UL (Mbps)	Peak Throughput DL (Mbps)
Sim.	2 ms	14,85	83,67
Sim.	5 ms	20,14	83,12
Sim.	10 ms	18,26	82,36
Theor.	5 ms	22,52	82,64
Lab.	5 ms	9,26	64,4

Table 11 shows the peak throughput for UL and DL traffic with a TDD pattern with 7 slots for DL traffic, 2 slots for UL traffic and 1 FL slot. Although the simulated and theoretical results match, the experimental ones do not, as they differ by approximately between 10 - 20 Mbps for UL and DL traffic, respectively. This is due to the automatic modulation selection by the OAI core based on the IQ value. It is worth noting the contrast between the experimental results and those obtained in the simulation. The experimental results for UL traffic were obtained using a BPSK modulation with a spectral efficiency of 1.03 [40], whereas for DL traffic the modulation used was 64-QAM with a spectral efficiency of 5.55 [40], which is different from the modulations used in the use case modelling; 64-QAM for UL traffic and 256-QAM for DL traffic. Furthermore, it is observed that the modification of the radio resource allocation of the 5G network does not greatly affect the E2E latency of the network when comparing the experimental results in Tables 7 and 10. On the other hand, the peak throughput is affected regardless of the traffic type, increasing to 83 Mbps peak throughput for DL traffic and decreasing to 20 Mbps for UL traffic using the resource allocation detailed in Table 6.

Finally, Fig. 12 shows the PDR achieved by message size for each of the transfer intervals used, differentiating between the two traffic types. Due to the allocation of radio resources in favour of DL traffic, better operating thresholds are achieved for one type of traffic than for the other. For example, for a transfer interval of 5 ms, the maximum packet size for UL traffic is 200 B, whereas for DL traffic, it is 1 KB, a packet size five times larger.

TABLE 12. E2E latency / PDR lab results for TDD pattern 3 DL / 6 UL / 1 FL.

E2E latency			PDR (%)
Minimum	Average	Maximum	
6,75	10,12	15,02	100

Figs. 13 and 14 and Tables 12 and 13 show the results of simulations with the following TDD frame configuration: 3 slots for DL traffic, 6 slots for UL traffic and 1 FL slot. The operating threshold for the above TDD pattern shows an E2E latency of less than 10 ms for a packet size of 500B and a transfer interval of 10 ms. Note that with this slot format, as with the previous one, no operational threshold is achieved with a transfer interval of less than 10 ms, so it is ruled out that these slot formats comply with E2E latency requirements for ultra-low latency services. On the other hand, it is observed that when the developed industrial use case deals only with DL traffic, DL latency results between 2 - 3 ms are obtained for small packet sizes and transfer intervals are obtained. Furthermore, the experimental E2E latency does not vary according to the TDD pattern used, as shown in Tables 10 and 12.

TABLE 13. Peak throughput for TDD pattern 3 DL / 6 UL / 1 FL.

Sim. / Theor. / Lab.	Transfer interval (ms)	Peak Throughput UL (Mbps)	Peak Throughput DL (Mbps)
Sim.	2 ms	59,77	23,85
Sim.	5 ms	61,56	24,14
Sim.	10 ms	67,19	21,92
Theor.	5 ms	66,3	20,07
Lab.	5 ms	10	16,3

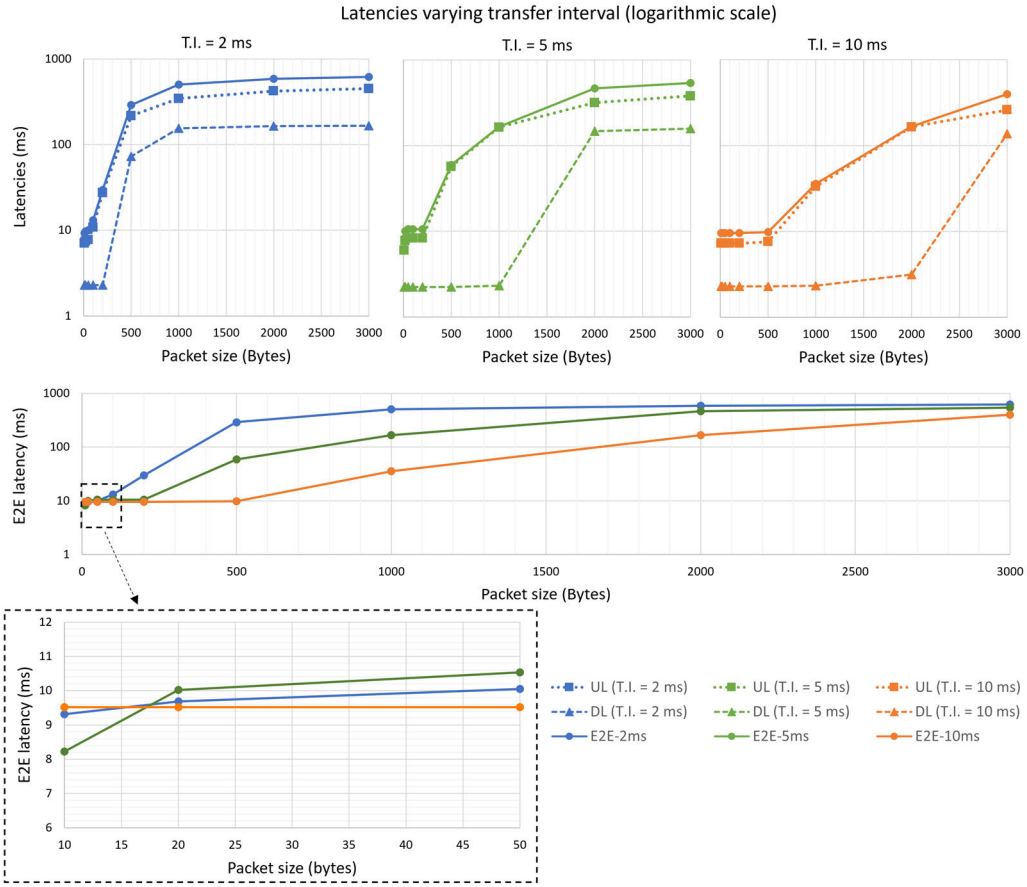

FIGURE 11. (Sim.) latencies for TDD pattern 7 DL / 2 UL / 1 FL.

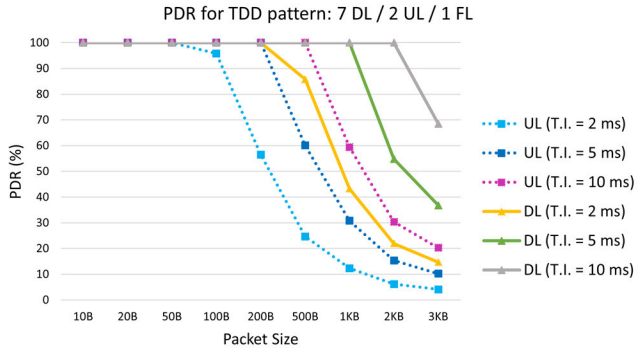

FIGURE 12. (Sim.) packet delivery ratio depending on the type of traffic for TDD pattern 7 DL / 2 UL / 1 FL.

As in the previous tests, there is a significant difference between the simulated and experimental laboratory results for UL traffic, while they are similar for DL traffic. This is because the modulation used in the laboratory tests is different from that used in both simulations and theoretical calculations. The experimental results were obtained using a BPSK modulation with a spectral efficiency of 1.33 [40] for UL traffic, while for DL traffic a 64-QAM modulation with a spectral efficiency of 4.82 [40] was used.

Finally, Fig. 14 shows the PDR obtained as a function of message size for the three transfer intervals used, differentiating the results by traffic type.

On the one hand, in the case of an industrial application characterised by DL traffic, the maximum packet size is 500 B for a transfer interval of 10 ms. On the other hand, if the industrial use case had the sole requirement of optimising resources for UL traffic, as is achieved with this TDD pattern, the maximum packet size is 2 KB for a 10 ms transfer interval and the maximum packet size is halved for a 5 ms transfer interval.

Summarising this second experimental test, detailed in Table 6, it can be observed that E2E latency does not depend on the radio resource allocation, but UL/DL latency does depend on the TDD pattern used. Furthermore, for small message sizes where the 5G network is not saturated, the modulation used has a greater impact, while when the network is saturated, the TDD pattern dominates. As shown in Fig. 13, for small message sizes, DL latency is lower than UL latency even when a TDD pattern is used in favour of UL traffic. However, when the network is saturated, the DL latency is higher than the UL latency.

Finally, as demonstrated in the testbed set, the correct allocation of radio resources must be made according to the

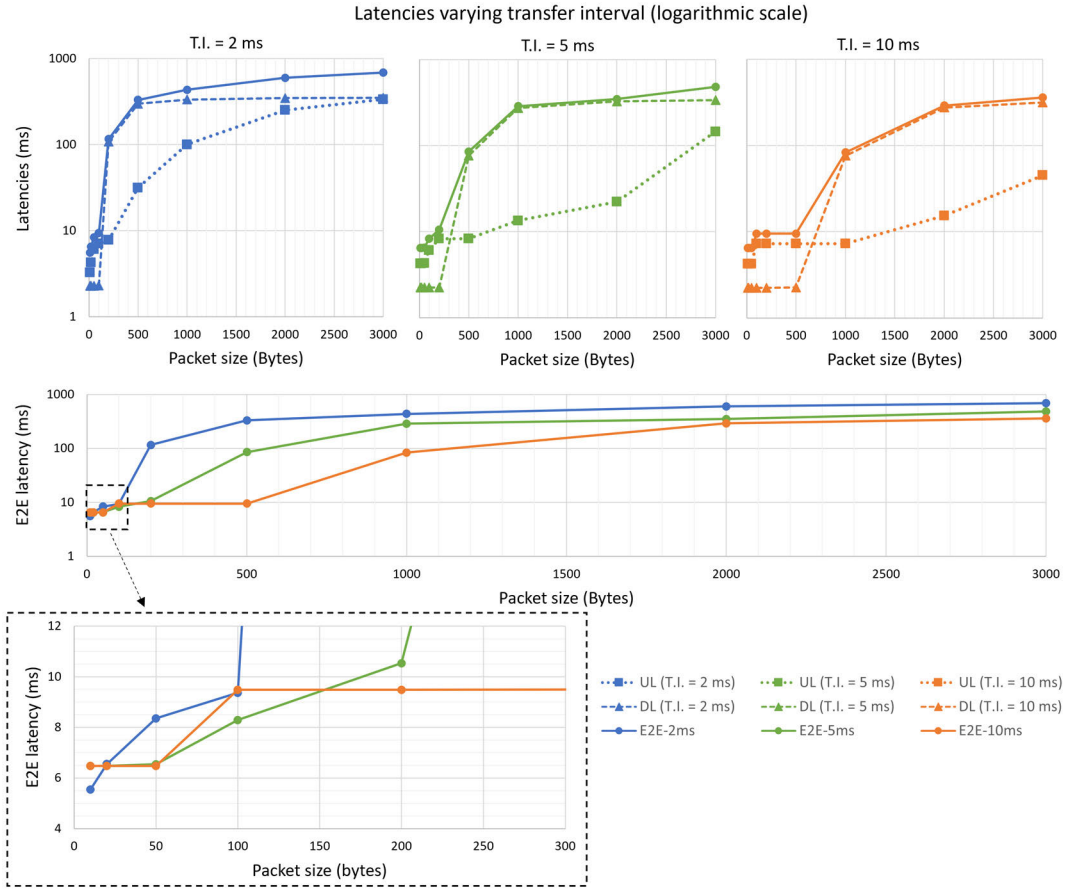

FIGURE 13. (Sim.) latencies for TDD pattern 3 DL / 6 UL / 1 FL.

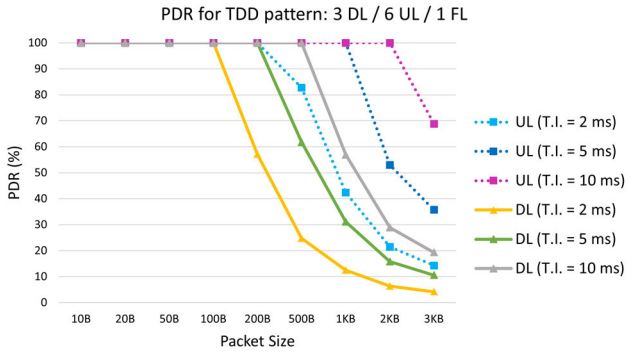

FIGURE 14. (Sim.) packet delivery ratio depending on the type of traffic for TDD pattern 3 DL / 6 UL / 1 FL.

traffic requirements of the industrial use case, as operational thresholds vary widely.

VII. CONCLUSION AND FUTURE WORK

Analysis of the operational thresholds of the two European sub-GHz spectrum reservation initiatives highlights the performance limitations of private 5G networks in industrial environments. Much effort is currently being put into the design and optimisation of features and models to improve the performance of private 5G networks, but the trend is towards the development of hybrid 5G networks due to the high installation costs. Moreover, given that homogeneous spectrum reserves for private 5G networks have not been established in European countries, which have taken the initiative to have large spectrum reserves in the n78 band, such as Germany, Poland, the UK, Switzerland or Sweden, among others, are achieving higher yields with the potential to make significant progress or develop new industrial applications than countries such as Finland, France or Spain, which have spectrum reserves in the n40 band, which has a much lower bandwidth than the n78 band.

Due to the examination of the operational thresholds following different radio resource configurations in the n40 band, it was found that the most restrictive spectrum initiative presents very limited network performance for use in industrial applications, as it presents an average E2E latency of 10 ms which may be insufficient for certain use cases detailed by 3GPP URLLC requirements. In terms of peak throughput, the results are similar to other wireless technologies, highlighting the resilience of medium and long distance communications. Therefore, it is possible to claim that private 5G networks are one of the emerging wireless technologies for implementation in industrial factories.

Finally, this work has provided an analysis of the performance of a private 5G network in both the n40 and n78 bands, although it has not detailed the spectrum pool with the most

performance limitations. It has also shown that the operating thresholds vary depending on the spectrum reserve used. Optimal configurations have also been evaluated and verified according to the type of application traffic, concluding that E2E latency is not modified by the allocation of radio resources, but by the modulation used for each type of traffic.

Therefore, several trends are emerging towards hybrid ecosystems combining different wireless technologies or towards public-private infrastructures, depending on the industrial requirements of each use case.

REFERENCES

[1] P. K. R. Maddikunta, Q.-V. Pham, N. Deepa, K. Dev, T. R. Gadekallu, R. Ruby, and M. Liyanage, "Industry 5.0: A survey on enabling technologies and potential applications," *J. Ind. Inf. Integr.*, vol. 26, Mar. 2022, Art. no. 100257, doi: 10.1016/j.jii.2021.100257.

[2] S. Misra, C. Roy, T. Sauter, A. Mukherjee, and J. Maiti, "Industrial Internet of Things for safety management applications: A survey," *IEEE Access*, vol. 10, pp. 83415–83439, 2022, doi: 10.1109/ACCESS.2022.3194166.

[3] E. Mozaffariahrar, F. Theoleyre, and M. Menth, "A survey of Wi-Fi 6: Technologies, advances, and challenges," *Future Internet*, vol. 14, no. 10, p. 293, Oct. 2022, doi: 10.3390/fi14100293.

[4] R. Maldonado, A. Karstensen, G. Pocovi, A. A. Esswie, C. Rosa, O. Alanen, M. Kasslin, and T. Kolding, "Comparing Wi-Fi 6 and 5G downlink performance for industrial IoT," *IEEE Access*, vol. 9, pp. 86928–86937, 2021, doi: 10.1109/ACCESS.2021.3085896.

[5] E. J. Oughton, W. Lehr, K. Katsaros, I. Selinis, D. Bubley, and J. Kusuma, "Revisiting wireless internet connectivity: 5G vs Wi-Fi 6," *Telecommun. Policy*, vol. 45, no. 5, Jun. 2021, Art. no. 102127, doi: 10.1016/j.telpol.2021.102127.

[6] A. Adel, "Future of industry 5.0 in society: Human-centric solutions, challenges and prospective research areas," *J. Cloud Comput.*, vol. 11, no. 1, p. 40, Sep. 2022, doi: 10.1186/s13677-022-00314-5.

[7] M. Wollschlaeger, T. Sauter, and J. Jasperneite, "The future of industrial communication: Automation networks in the era of the Internet of Things and industry 4.0," *IEEE Ind. Electron. Mag.*, vol. 11, no. 1, pp. 17–27, Mar. 2017, doi: 10.1109/MIE.2017.2649104.

[8] S.-Y. Lien, S.-L. Shieh, Y. Huang, B. Su, Y.-L. Hsu, and H.-Y. Wei, "5G new radio: Waveform, frame structure, multiple access, and initial access," *IEEE Commun. Mag.*, vol. 55, no. 6, pp. 64–71, Jun. 2017.

[9] S. Eswaran and P. Honnavalli, "Private 5G networks: A survey on enabling technologies, deployment models, use cases and research directions," in *Telecommunication Systems*, vol. 82, 2023, doi: 10.1007/s11235-022-00978-z.

[10] GSMA. (Oct. 2020). *5G Private & Dedicated Networks for Industry 4.0*. Accessed: Feb. 2023. [Online]. Available: https://www.gsma.com/iot/resources/5g-private-npn-industry40/

[11] 3GPP. (Oct. 2022). *NR and NG-RAN Overall Description (Release 17), Technical Specification TS 38.300 v17.2.0*. Accessed: Nov. 2022. [Online]. Available: https://www.etsi.org/deliver/etsi_ts/138300_138399/138300/17.02.00_60/ts_138300v170200p.pdf

[12] P. Mishra, S. Kar, V. Bollapragada, and K.-C. Wang, "Multi-connectivity using NR-DC for high throughput and ultra-reliable low latency communication in 5G networks," in *Proc. IEEE 4th 5G World Forum (5GWF)*, Oct. 2021, pp. 36–40, doi: 10.1109/5GWF52925.2021.00014.

[13] 3GPP. (Dec. 2021). *Service Requirements for Cyber-Physical Control Applications in Vertical Domains (Release 18), Technical Specification TS 22.104 v18.3.0*. Accessed: Dec. 2022. [Online]. Available: https://portal.3gpp.org/desktopmodules/Specifications/SpecificationDetails.aspx?specificationId=3528

[14] L. M. Bartolín-Arnau, J. Vera-Pérez, V. M. Sempere-Payá, and J. Silvestre-Blanes, "Private 5G networks for cyber-physical control applications in vertical domains," in *Proc. IEEE 19th Int. Conf. Factory Commun. Syst. (WFCS)*, Apr. 2023, pp. 1–4.

[15] M. K. Müller, F. Ademaj, T. Dittrich, A. Fastenbauer, B. R. Elbal, A. Nabavi, L. Nagel, S. Schwarz, and M. Rupp, "Flexible multi-node simulation of cellular mobile communications: The Vienna 5G system level simulator," *EURASIP J. Wireless Commun. Netw.*, vol. 2018, no. 1, p. 227, Dec. 2018, doi: 10.1186/s13638-018-1238-7.

[16] Y. Kim, J. Bae, J. Lim, E. Park, J. Baek, S. I. Han, C. Chu, and Y. Han, "5G K-simulator: 5G system simulator for performance evaluation," in *Proc. IEEE Int. Symp. Dyn. Spectr. Access Netw. (DySPAN)*, Oct. 2018, pp. 1–2, doi: 10.1109/DySPAN.2018.8610404.

[17] N. Patriciello, S. Lagen, B. Bojovic, and L. Giupponi, "An E2E simulator for 5G NR networks," 2019, *arXiv:1911.05534*.

[18] S. Martiradonna, "5G-air-simulator: An open-source tool modeling the 5G air interface," *Comput. Netw.*, vol. 173, May 2020, Art. no. 107151.

[19] G. Pereyra, C. Rattaro, and P. Belzarena, "Py5cheSim: A 5G multi-slice cell capacity simulator," in *Proc. XLVII Latin Amer. Comput. Conf. (CLEI)*, Cartago, Costa Rica, Oct. 2021, pp. 1–8, doi: 10.1109/CLEI53233.2021.9640086.

[20] G. Nardini, G. Stea, A. Virdis, and D. Sabella, "Simu5G: A system-level simulator for 5G networks," in *Proc. 10th Int. Conf. Simul. Model. Methodologies, Technol. Appl.*, 2020, pp. 68–80, doi: 10.5220/0009826400680080.

[21] S. Kar, P. Mishra, and K.-C. Wang, "5G-IoT architecture for next generation smart systems," in *Proc. IEEE 4th 5G World Forum (5GWF)*, Oct. 2021, pp. 241–246, doi: 10.1109/5GWF52925.2021.00049.

[22] T. Cogalan et al., "5G-CLARITY: 5G-advanced private networks integrating 5GNR, WiFi, and LiFi," *IEEE Commun. Mag.*, vol. 60, no. 2, pp. 73–79, Feb. 2022, doi: 10.1109/mcom.001.2100615.

[23] C. Arendt, "Empowering the convergence of Wi-Fi and 5G for future private 6G networks," in *Proc. Eur. Wireless 28th Eur. Wireless Conf.*, 2023.

[24] G. Nardini, G. Stea, A. Virdis, D. Sabella, and P. Thakkar, "Using Simu5G as a realtime network emulator to test MEC apps in an end-to-end 5G testbed," in *Proc. IEEE 31st Annu. Int. Symp. Pers., Indoor Mobile Radio Commun.*, Aug. 2020, pp. 1–7.

[25] A. Noferi, G. Nardini, G. Stea, and A. Virdis, "Deployment and configuration of MEC apps with Simu5G," 2021, *arXiv:2109.12048*.

[26] A. Noferi, G. Nardini, G. Stea, and A. Virdis, "Rapid prototyping and performance evaluation of ETSI MEC-based applications," *Simul. Model. Pract. Theory*, vol. 123, Feb. 2023, Art. no. 102700, doi: 10.1016/j.simpat.2022.102700.

[27] A. Virdis, "End-to-end performance evaluation of MEC deployments in 5G scenarios," *Sensor Actuator Netw.*, vol. 9, no. 4, p. 57, Dec. 2020.

[28] S. Jaeckel, N. Turay, L. Raschkowski, L. Thiele, R. Vuohtoniemi, M. Sonkki, V. Hovinen, F. Burkhardt, P. Karunakaran, and T. Heyn, "Industrial indoor measurements from 2–6 GHz for the 3GPP-NR and QuaDRiGa channel model," in *Proc. IEEE 90th Veh. Technol. Conf. (VTC-Fall)*, Honolulu, HI, USA, Sep. 2019, pp. 1–7, doi: 10.1109/VTC-Fall.2019.8891356.

[29] C. Bektas, C. Schüler, R. Falkenberg, P. Gorczak, S. Böcker, and C. Wietfeld, "On the benefits of demand-based planning and configuration of private 5G networks," in *Proc. IEEE Veh. Netw. Conf. (VNC)*, Ulm, Germany, Nov. 2021, pp. 158–161, doi: 10.1109/VNC52810.2021.9644659.

[30] M. Wen, Q. Li, K. J. Kim, D. López-Pérez, O. A. Dobre, H. V. Poor, P. Popovski, and T. A. Tsiftsis, "Private 5G networks: Concepts, architectures, and research landscape," *IEEE J. Sel. Topics Signal Process.*, vol. 16, no. 1, pp. 7–25, Jan. 2022, doi: 10.1109/JSTSP.2021.3137669.

[31] European Commission. *5G Action Plan*. Accessed: Nov. 2022. [Online]. Available: https://digital-strategy.ec.europa.eu/en/policies/5g-action-plan

[32] G. Nardini, D. Sabella, G. Stea, P. Thakkar, and A. Virdis, "Simu5G–An OMNeT++ library for end-to-end performance evaluation of 5G networks," *IEEE Access*, vol. 8, pp. 181176–181191, 2020, doi: 10.1109/ACCESS.2020.3028550.

[33] R. G. Lazar, C. F. Caruntu, and C. Patachia-Sultanoiu, "Simulated and practical approach to assess the reliability of the 5G communications for the Uu interface," in *Proc. 14th Int. Conf. Commun. (COMM)*, Jun. 2022, pp. 1–6, doi: 10.1109/COMM54429.2022.9817312.

[34] 3GPP, "Summary of Rel-15 work items (release 15)," Tech. Rep. TR 21.915 v15.0.0, Oct. 2019, Accessed: Nov. 2022. [Online]. Available: https://portal.3gpp.org/desktopmodules/Specifications/SpecificationDetails.aspx?specificationId=3389

[35] *5G NR Numerology—Terminology*. Accessed: Nov. 2022. [Online]. Available: https://www.rfwireless-world.com/5G/5G-NR-Numerology-or-Terminology.html

[36] *User Equipment (UE) Radio Transmission and Reception (Release 17)*, 3GPP, document Technical Specification TS 38.101-1, V17.7.0, Oct. 2022. Accessed: Jan. 2023. [Online]. Available: https://portal.3gpp.org/desktopmodules/Specifications/SpecificationDetails.aspx?specificationId=3283

[37] *User Equipment (UE) Radio Access Capabilities (Release 17)*, 3GPP, document Technical Specification TS 38.306, v17.5.0, Sep. 2023.
[38] 3GPP, "Study on new radio access technology: Physical layer aspects (release 14)," Tech. Rep. TR 38.802, v14.2.0, Sep. 2017, Accessed: Jun. 2023. [Online]. Available: https://portal.3gpp.org/desktopmodules/Specifications/SpecificationDetails.aspx?specificationId=3066
[39] *Multiplexing and Channel Coding (Release 15)*, 3GPP, document Technical Specification TS 38.212, v17.5.0, Mar. 2023, Accessed: Jul. 2023. [Online]. Available: https://portal.3gpp.org/desktopmodules/Specifications/SpecificationDetails.aspx?specificationId=3214
[40] *Physical Layer Procedures for Data (Release 17)*, 3GPP, document Technical Specification TS 38.214, v17.6.0, Accessed: Jun. 2023. [Online]. Available: https://portal.3gpp.org/desktopmodules/Specifications/SpecificationDetails.aspx?specificationId=3216
[41] *Technical Channels and Modulation (Release 17)*, 3GPP, document Technical Specification TS 38.211, v17.5.0, Jul. 2023. [Online]. Available: https://portal.3gpp.org/desktopmodules/Specifications/SpecificationDetails.aspx?specificationId=3213
[42] *Service Requirements for the 5G System (Release 19)*, 3GPP, document Techinical Specification TS 22.261, v19.2.0, Mar. 2023. [Online]. Available: https://portal.3gpp.org/desktopmodules/Specifications/SpecificationDetails.aspx?specificationId=3107
[43] C. Casetti, "5G consolidates deployment by targeting new bands [mobile radio]," *IEEE Veh. Technol. Mag.*, vol. 16, no. 4, pp. 6–11, Dec. 2021, doi: 10.1109/MVT.2021.3116735.
[44] X. An. (Nov. 2020). *5G Industry Campus Network Deployment Guideline v1.0*. Accessed: Dec. 2022. [Online]. Available: https://www.gsma.com/newsroom/wp-content/uploads/NG.123-v1.0-3.pdf
[45] *OMNeT++*. Accessed: Nov. 2022. [Online]. Available: https://omnetpp.org/
[46] L. F. Perrone, C. Cicconetti, G. Stea, and B. C. Ward, "On the automation of computer network simulators," in *Proc. 2nd Int. ICST Conf. Simul. Tools Techn.*, 2009, pp. 1–10.
[47] *INET Library*. Accessed: Oct. 2022. [Online]. Available: https://inet.omnetpp.org/
[48] *Summary of Rel-16 Work Items (Release 16)*, 3GPP, document Technical Specification TS 21.916, v16.2.0, Nov. 2022, https://portal.3gpp.org/desktopmodules/Specifications/SpecificationDetails.aspx?specificationId=3493
[49] 3GPP, "Study on communication for automation in vertical domains (release 16)," Tech. Rep. TR 22.804, v16.3.0, Jun. 2020, Accessed: May 2023. [Online]. Available: https://portal.3gpp.org/desktopmodules/Specifications/SpecificationDetails.aspx?specificationId=3187
[50] 3GPP, "Study on channel model for frequencies from 0.5 to 100 GHz (release 17)," Tech. Rep. TR 38.901, v17.0.0, Mar. 2022, Accessed: Jul. 2023. [Online]. Available: https://portal.3gpp.org/desktopmodules/Specifications/SpecificationDetails.aspx?specificationId=3173
[51] Open Air Interface (OAI). *OpenAirInterface Software Alliance*. [Online]. Available: https://github.com/openairinterface

LUIS M. BARTOLÍN-ARNAU received the degree in telecommunications engineering. He is currently pursuing the M.Sc. degree in big data analytics. Prior to this, he worked on different home automation projects as well as the implementation of LPWAN technologies in rural areas in Spain for two years. He is a Research Engineer with the Advanced Communications Research Group, Instituto Tecnológico de Informática (ITI). His current research interest includes the design, evaluation, and implementation of edge computing to reduce cloud computing costs in the IoT devices.

JOSE VERA-PÉREZ was born in Lorca, Murcia, Spain, in 1993. He received the B.S. and M.S. degrees in telecommunications engineering from Universitat Politècnica de València (UPV), Spain, in 2017, and the Ph.D. degree in telecommunication engineering, with a focus on optimization mechanism for industrial wireless sensor networks. He is currently a Research and Development Engineer with the Advanced Communication and Industrial Informatics Group, Instituto Tecnológico de Informática (ITI), Valencia. He is the author of several recent research related to wireless sensor networks for industrial communications. His research interests include private 5G networks, low-power wireless communications, Industry 4.0, industrial automation, and cybersecurity.

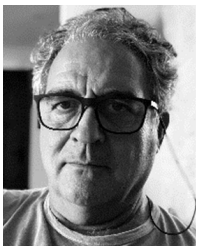

VÍCTOR SEMPERE-PAYÁ (Member, IEEE) received the first degree in industrial electronics, the second degree in computer engineering, and the Ph.D. degree in telecommunications engineering from Universitat Politècnica de València (UPV), Valencia, Spain, in 1987, 1993, and 1998, respectively. He is currently an Associate Professor with the Department of Communications, UPV, where he teaches industrial communications and public access networks. He is also the Director of the Advanced Communications and Industrial Informatics Group, Instituto Tecnológico de Informática (ITI). Since 1996, he has authored or coauthored more than 60 technical papers in journals and international conferences. He has managed more than 50 research and technological projects. His current research interests include factory communications, real-time communications, and quality of service (QoS) in networks. He has served as a program committee member for several conferences in the area of factory communications.

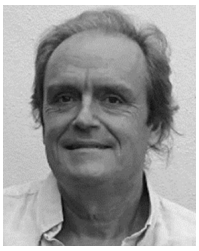

JAVIER SILVESTRE-BLANES (Member, IEEE) was born in Alcoy, Valencia, Spain, in 1965. He received the M.S. and Ph.D. degrees in computer architecture, in 1999 and 2003, respectively. In 1999, he joined the Department of Computer Architecture, Universitat Politècnica de València, as a part-time Associate Lecturer, where he was promoted to an Assistant Lecturer, in 2004, and has been an Associate Professor, since 2010. In 2009, he joined the Instituto Tecnológico de Informática (ITI), where his research and development area (industrial computing, communications, and image processing), participating in research and development projects both individually and in cooperation with other entities. He has more than 34 papers in international peer-reviewed conferences, 28 articles published in journals of impact JCR, and eight book chapters, related to the sector of industrial communications, heterogeneous networks, multimedia networks, image processing, and computer vision. He has carried out research stays abroad, with the University of Aveiro, Portugal, and Anglia Ruskin University, Cambridge, U.K. He is a member of the Industrial Electronics Society (IES), belonging to the IEEE, where he also belongs to the Sub-Committee FA10 Computer Vision and Human–Machine Interaction in Industrial and Factory Automation, belonging to the IES-IEEE Factory Automation Committee. Since 2005, he has been participated as a member of the organizing committee or a member of the program committee of numerous international conferences of the IEEE Industrial Electronics Society.